

# The parity determination of the pentaquark $\Lambda^+$ from photoproduction near threshold

Byung Geel Yu,<sup>1,2</sup> Tae Keun Choi,<sup>3,y</sup> and Chueng-Ryong Ji<sup>2,z</sup>

<sup>1</sup>Department of General Studies, Hangeong Aviation University, Koyang, 200-1, Korea

<sup>2</sup>Department of Physics, North Carolina State University,  
Raleigh, North Carolina 27695-8202, USA

<sup>3</sup>Department of Physics, Yonsei University, Wonju, 220-710, Korea

(Dated: December 22, 2018)

## Abstract

We discuss how the angular distribution and the photon polarization asymmetry for the reaction  $N \rightarrow K^+ \Lambda^+$  can be used to determine the parity of the  $\Lambda^+$  unambiguously by the conservation laws of the parity and angular momentum incorporated with the threshold kinematics of the reaction near threshold. Using the general form of the spin structures of the process, we present a consistency of our description.

PACS numbers: 13.40.-f, 13.60.Rj, 13.75.Jz, 13.88.+e

Keywords:  $\Lambda^+$  parity, photoproduction, angular distribution, parity and angular momentum conservations, photon polarization asymmetry

---

<sup>1</sup>Electronic address: bgyu@mailhangkong.ac.kr

<sup>y</sup>Electronic address: tkchoi@dragon.yonsei.ac.kr

<sup>z</sup>Electronic address: crji@unity.ncsu.edu

## 1. Introduction

The experimental evidences of the pentaquark  $\Sigma^+$  baryon have been growing since the observation of the narrow peak reported from the experiments in Refs. [1, 2, 3, 4, 5, 6, 7, 8]. To investigate the properties of the  $\Sigma^+$  further, the determination of its parity is crucial because it is a decisive quantum number to understand the substructure of the new resonance with the strangeness  $S = +1$  [9, 10].

In Ref. [11] and the subsequent works [12, 13], the conservation laws were applied to give strong constraints on the parity and total angular momentum of the initial state in the polarized process  $pp \rightarrow \Sigma^+ \Sigma^+$  near threshold. The parity of  $\Sigma^+$  has been claimed to be clearly determined as a consequence of the Fermi statistics of two-nucleon system. Also, Ref. [14] suggested that the parity of  $\Sigma^+$  can be determined model-independently by observing the polarization asymmetries based on the reflection symmetry of the polarized process  $N \rightarrow K \Sigma^+$ . In addition, Refs. [15, 16, 17] proposed to use the polarized photon beam for the process  $N \rightarrow K \Sigma^+$  to determine the  $\Sigma^+$  parity model-independently. These works emphasize that the polarization observables are important tools to determine the  $\Sigma^+$  parity.

In this paper, however, we note that the first principle conservation laws of the parity and angular momentum can also be exploited for the unpolarized observable to clarify the  $\Sigma^+$  parity as far as the photon energy is near threshold in the photoproduction process. We discuss the role of the parity and angular momentum conservations on the process  $N \rightarrow K \Sigma^+$  in detail and show that it is possible to describe the threshold amplitude of the process from the first principle with the threshold kinematics. As a result, the two opposite parity states of the  $\Sigma^+$  can be distinguishable from each other by analyzing simply the angular distribution of the unpolarized photoproduction process. We can also extend our analysis to the polarization observable and make a prediction for the photon polarization asymmetry. Of course this sort of observation in the photoproduction process is not new but has been already applied to the pion photo and electroproduction processes near threshold extensively as shown in many literatures. Since the charge coupling structures of  $n \rightarrow K \Sigma^+$  and  $p \rightarrow K \Sigma^0$  are very similar to those of  $n \rightarrow p$  and  $p \rightarrow \Sigma^0$ , respectively, in the Born approximation amplitudes, we utilize the analogy of the pion photoproduction near threshold.

For explicit quantitative predictions (e.g. angular distributions), we present the numerical results of the angular distribution and photon polarization asymmetry by utilizing the hadron model presented in Ref. [18]. The model dependence in this case, however, can be minimized near

TABLE I: Multipole states for  $N \rightarrow K^+$ . For the transverse photon states,  $L = 1$ .

L	Positive parity				Negative parity			
	EL (ML)	$J^P$	l	multipoles	EL (ML)	$J^P$	l	multipoles
1	E1	$\frac{1}{2}$	0	$E_{0+}$	M1	$\frac{1}{2}^+$	0	$M_{0+}$
1	M1	$\frac{1}{2}^+$	1	$M_{1-}$	E1	$\frac{1}{2}$	1	$E_{1-}$
1	M1	$\frac{3}{2}^+$	1	$M_{1+}$	E1	$\frac{3}{2}$	1	$E_{1+}$
2	E2	$\frac{3}{2}^+$	1	$E_{1+}$	M2	$\frac{3}{2}$	1	$M_{1+}$

threshold because only the lower angular momentum states are available and, thus, it is rather easy to implement the first principle conservation laws.

In Section 2, we present our reasoning for the difference in the angular distribution depending on the parity of  $K^+$ . The CGLN amplitudes are also used to discuss the consistency of our description. In Section 3, we extend our analysis to the photon polarization asymmetry. Summary and discussion follows in Section 4.

## 2. Angular Distribution

In the threshold region it is legitimate to assume that the kaon angular momentum  $l = 0$  or  $1$  in the  $n\pi K^+$  state, since  $\frac{p}{\hbar} \approx \frac{p}{197 \text{ MeV}/c} \approx 2$  up to a few hundred MeV/c of the kaon momentum  $p$  in the center of mass (CM) frame with  $R$ , a typical hadronic scale of one fermi. The angular momentum of the  $n\pi$  state can have either  $J = \frac{1}{2}$  or  $\frac{3}{2}$ , and the parity of the  $n\pi$  state is given by  $(-1)^{l+1}$  for  $(\frac{1}{2}^+)$  or  $(-1)^l$  for  $(\frac{1}{2}^-)$ . The angular momentum of the initial  $N$  state,  $J = \frac{1}{2}$  and the state has the parity, either  $(-1)^L$  for electric or  $(-1)^{L+1}$  for magnetic, where  $L$  is the total angular momentum of the photon [19, 20]. Then, from the conservation of parity and angular momentum, only the s- and p-waves are likely as shown in Table I. Near threshold, however, the E1 transition must be dominant over the M1 transition in general. Also the lower  $J$  state (i.e.,  $J = \frac{1}{2}$ ) must be energetically more easily accessible than the higher  $J$  state (i.e.,  $J = \frac{3}{2}$ ). Therefore, unless some other particular reasons, one may expect that  $E_{0+}$  and  $E_{1-}$  transitions are dominant near threshold for the positive and negative parity  $K^+$ , respectively. This would lead to a rather clear difference in the angular distributions for the  $N \rightarrow K^+$  process depending on the  $K^+$  parity. We show in this work that this general expectation holds for the  $n\pi K^+$  case while the  $p\pi K^0$  case doesn't share the same expectation due to the absence of the charge coupling of photon to the neutral meson.

For the consistency check of our description, let us now expand the photoproduction operator in terms of the CGLN amplitudes [21]. In the case of  $^{+}(\frac{1}{2}^+)$ , the CGLN amplitude is given by

$$J^+ = F_1^+ i \hat{k} \cdot \hat{q} + F_2^+ \hat{q} \cdot (\hat{k} \times \hat{q}) + F_3^+ i \hat{k} \cdot \hat{q} \hat{q} \cdot \hat{k} + F_4^+ i \hat{q} \cdot \hat{q} \hat{k} \cdot \hat{q} \quad (1)$$

where  $\hat{k}, \hat{q}$  are the unit vectors of photon and kaon three momenta and  $\hat{e}$  is the photon polarization vector with polarization  $\lambda$ . Likewise, the expansion of the photoproduction operator for the  $^{+}(\frac{1}{2}^-)$  is given by [22]

$$J^- = F_1^- i \hat{k} \cdot \hat{q} + F_2^- \hat{q} \cdot (\hat{k} \times \hat{q}) + F_3^- i (\hat{q} \cdot \hat{k}) \hat{q} \cdot \hat{k} + F_4^- \hat{q} \cdot \hat{q} \hat{k} \cdot \hat{q} \quad (2)$$

The superscripts stand for the parities of  $^{+}$  in what follows. The CGLN amplitudes in Eqs. (1) and (2) are given by

$$\begin{aligned} F_1 &= \frac{k \cdot j}{4} N_+ A_1 - \frac{1}{2} (W - M) A_3 - \frac{p^0 \cdot k}{W - M} A_4 ; \\ F_2 &= \frac{k \cdot j}{4} N_- A_1 + \frac{1}{2} (W - M) A_3 + \frac{p^0 \cdot k}{W - M} A_4 ; \\ F_3 &= \frac{k \cdot j \cdot j}{4} N_+ (W - M) A_2 - A_4 ; \\ F_4 &= \frac{k \cdot j \cdot j}{4} N_- (W + M) A_2 + A_4 - \frac{(W + M) k \cdot q}{(E + M)(E - M)} A_2 - \frac{A_4}{W - M} ; \end{aligned} \quad (3)$$

with the normalization constant  $N = \frac{q}{E - M}$ . Here  $A_i$ 's are the invariant transition amplitudes.

We now note that the knowledge of the kinematics of CGLN amplitudes near threshold enables us to determine which amplitude gives the leading contribution to the currents  $J$  in Eqs.(1) and (2). First, the amplitudes  $F_2^+$  and  $F_4^+$  are substantially suppressed near threshold due to the kinematical constant  $N$  in Eq.(3). Therefore, the current of Eq.(1) near threshold can be written as  $J^+ \approx F_1^+ i \hat{k} \cdot \hat{q} + F_3^+ i \hat{k} \cdot \hat{q} \hat{q} \cdot \hat{k}$ . Similarly, the amplitudes  $F_2^-$  and  $F_3^-$  can be neglected near threshold and the current in Eq.(2) can be given by  $J^- \approx F_1^- i \hat{k} \cdot \hat{q} + F_4^- \hat{q} \cdot \hat{q} \hat{k} \cdot \hat{q}$ . At threshold, it is apparent that only the terms of  $i \hat{k} \cdot \hat{q}$  and of  $i \hat{k} \cdot \hat{q} \hat{q} \cdot \hat{k}$  in the currents  $J$  remain to produce the s-wave kaon for each positive and negative parity  $^{+}$ , respectively. Terms of the operators  $i \hat{k} \cdot \hat{q} \hat{q} \cdot \hat{k}$  and  $\hat{q} \cdot \hat{q} \hat{k} \cdot \hat{q}$  will produce the p-wave kaon just above threshold and these are governed by the t-channel kaon pole term in the case of charged kaon photoproduction. Thus, the multipoles allowed by the conservation laws in Table I are already reflected in these current operators near threshold.

In the multipole expansion of the CGLN amplitudes [19] of the charged meson photoproduction,  $n! K^{+}$ , the s-wave multipole  $E_{0+}$  is dominant and the p-wave multipole  $M_{1-}$  is usually small

near threshold for the positive parity  $^{+}$  as discussed above (see Table I). Similarly, the p-wave multipole  $E_1^{-}$  is dominant for negative parity  $^{-}$ . Specifically, the strength of  $F_1^{-}$  is smaller than that of  $F_4^{-}$  whereas the strength of  $F_1^{+}$  is larger than that of  $F_3^{+}$ , since the value for the amplitude  $F_1^{-}$  of  $i \hat{k} \cdot \hat{\epsilon}$  is suppressed near threshold by a kinematical factor of  $\frac{k}{(E+M)}$ , an order of magnitude smaller than that of  $i \hat{k} \cdot \hat{\epsilon}$  [22, 23]<sup>1</sup> compared to the positive parity case. Hence, the term of  $\hat{q} \cdot \hat{\epsilon}$  coupling to p-wave kaon gives more important contribution to  $^{+}(\frac{1}{2})$ .

In the case of  $p \rightarrow K^0 \gamma$ , however, the process contains only s- and u-channel pole terms due to the absence of the charge coupling of photon to the neutral meson. Therefore, the t-channel kaon pole contribution to the term  $F_4 \hat{q} \cdot \hat{\epsilon}$  is absent, and consequently the term  $F_1 i \hat{k} \cdot \hat{\epsilon}$  is the leading contribution to the threshold amplitude of  $^{+}(\frac{1}{2})$  similar to the positive parity case. But in this case of neutral meson photoproduction, there is no leading contribution to  $F_1^{-}$  from the Kroll-Ruderman term in the multipole expansion. Thus, unlike to the process  $n \rightarrow K^+ \gamma$ , the value for  $F_1^{+}$  in this case is small and the same order as  $F_1^{-}$ .

For comparison, we estimate the energy and angle dependence of the CGLN amplitudes  $F_i$  using the Born approximation amplitude of Ref. [18] with coupling constants given in Table II and present the results in Figs. 1 and 2. In Fig. 1 the suppression of  $F_1^{-}$  by an order of magnitude compared to  $F_1^{+}$  is well reproduced, which should not be regarded as a result of the model-dependence. The features of  $n \rightarrow K^+ \gamma$  are represented as the dominance of  $F_1^{+} i \hat{k} \cdot \hat{\epsilon}$  in the  $^{+}(\frac{1}{2})$  and of  $F_4 \hat{q} \cdot \hat{\epsilon}$  in the  $^{+}(\frac{1}{2})$  respectively by the conservation laws plus the threshold kinematics as shown in Fig. 1 (see the similar conclusion for  $n \rightarrow K^+ \gamma$  in Ref. [16]). Thus, they are consistent with our earlier model-independent discussion without referring much to the dynamical details of invariant amplitudes  $A_i$  which usually involve the model parameters of the reaction mechanism.

At this point it is worth noting that Ref. [15] also discussed the methods to determine the  $^{+}$  parity in a model independent way using the process  $N \rightarrow K^+ \gamma$ . Since they did not consider the kinematical factor of  $\frac{k}{E+M}$  which is important to suppress the amplitude of  $F_1^{-}$  in the case of  $n \rightarrow K^+ \gamma$  as discussed above, they started with the s-wave amplitude common to both parities of  $^{+}$ . They proposed instead to observe the spin observables more than the single and double polarizations, or use the depolarization tensor component to relate the spin observables to the

<sup>1</sup> The kinematical factor can be checked by the nonrelativistic reduction of the vertex  $K N \rightarrow \gamma(\frac{1}{2})$  in the CM frame,

$$V_{KN} = \frac{eg}{M} \frac{1}{M} u(p^0) = u(p) = \frac{eg}{M} \frac{1}{M} N N^0 \frac{\mathbf{k} \cdot \mathbf{j}}{E+M} \gamma_i \cdot \hat{\epsilon} +$$

with  $N(N^0)$  the normalization constant of initial (nal) Dirac spinor.

TABLE II: Coupling constants used in the calculation for  $n \rightarrow K^+ \bar{K}^0$ .  $\Gamma_{n \rightarrow K^+ \bar{K}^0} = 5 \text{ MeV}$  taken for  $g_{K^+ \bar{K}^0}$  of the  $^+ (\frac{1}{2}^-)$  [18]. References are from <sup>a</sup>the assumption [24], <sup>b</sup>PDG [25], <sup>c</sup> $p \rightarrow K^+ \bar{K}^0$  [26] where we assume  $e \frac{G_{K^+ \bar{K}^0}}{G_{K^+ \bar{K}^0}} \cdot \frac{G_{K^+ \bar{K}^0}^{(1116)}}{G_{K^+ \bar{K}^0}^{(1116)}}$  for  $^+ (\frac{1}{2}^+)$  and  $\frac{G_{K^+ \bar{K}^0}}{G_{K^+ \bar{K}^0}} \cdot \frac{G_{K^+ \bar{K}^0}^{(1405)}}{G_{K^+ \bar{K}^0}^{(1405)}}$  for  $^+ (\frac{1}{2}^-)$  with  $G_{K^+ (K^+ \bar{K}^0)}$  =  $g_{K^+ (K^+ \bar{K}^0)}$   $g_{K^+ (K^+ \bar{K}^0)}$ , and <sup>d</sup> $\Gamma_{K^+ \bar{K}^0} = 37.8 \text{ MeV}$  with Vector Dominance  $g_{K^+ \bar{K}^0} = \frac{e}{f} g_{K^+ \bar{K}^0}$  [27]. Values in the parenthesis are denoted by  $n \rightarrow K^+ \bar{K}^0$  ( $p \rightarrow K^+ \bar{K}^0$ ) respectively.

	Positive parity	Negative parity	References
$g_{K^+ \bar{K}^0}$	2.2	0.3	$n \rightarrow K^+ \bar{K}^0$
$g_{K^+ \bar{K}^0}$	1.32	0.18	$\frac{g_{K^+ \bar{K}^0}}{g_{K^+ \bar{K}^0}} = 0.6^a$
$g_{K^+ \bar{K}^0}$	0.254 (0.388)	0.254 (0.388)	$K^+ \rightarrow K^+ \bar{K}^0$ <sup>b</sup>
$g_{K^+ \bar{K}^0}$	0.07 (0.1)	0.1 (0.16)	$\frac{G_{K^+ \bar{K}^0}^{(1116)}}{G_{K^+ \bar{K}^0}^{(1116)}}$ , $8^c$ $\frac{G_{K^+ \bar{K}^0}^{(1405)}}{G_{K^+ \bar{K}^0}^{(1405)}}$ , $0.7^c$
$g_{K^+ \bar{K}^0}$	0.6	0.6	$g_{K^+ \bar{K}^0}$ <sup>d</sup>

unpolarized cross section for the model-independent analysis. This makes a difference from our prediction in the case of  $n \rightarrow K^+ \bar{K}^0$ . As we pointed out, just above the threshold our amplitudes in this case are dominated by the s- and p-wave amplitudes for the positive and negative parity, respectively, and hence yield the angular distribution different from each other.

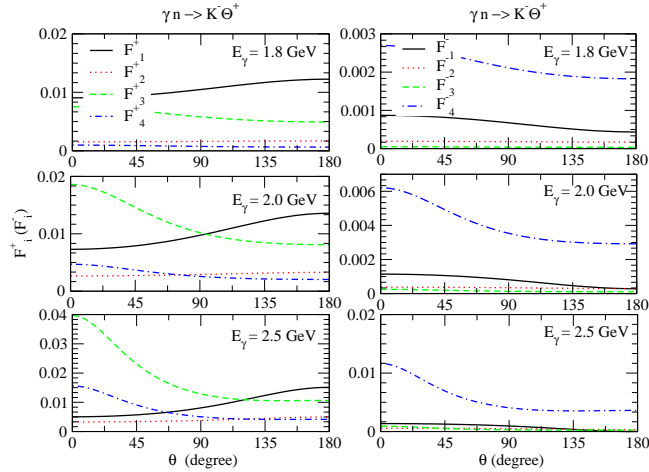


FIG. 1: Angle and energy dependence of the CGLN amplitudes  $F_i^+$ 's for  $^+ (\frac{1}{2}^+)$  (left) and  $F_i^-$ 's for  $^+ (\frac{1}{2}^-)$  (right) in the  $n \rightarrow K^+ \bar{K}^0$ .

We now analyze the angular distribution. Defining

$$\frac{d}{d\Omega} = \frac{1}{4\pi} \frac{d}{d\cos\theta} \quad (4)$$

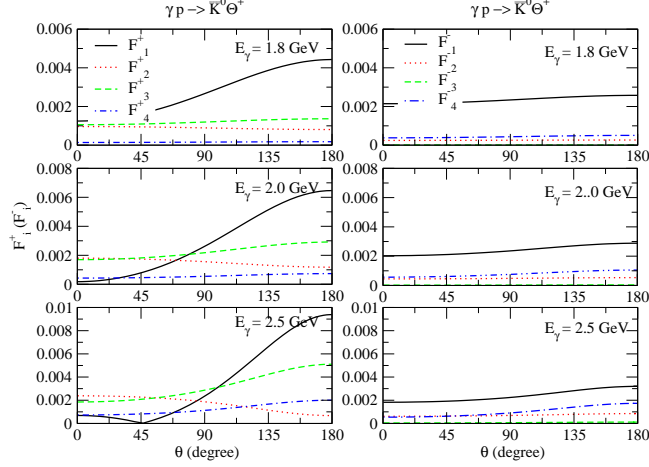


FIG. 2: Angle and energy dependence of the amplitudes  $F_i^+$  for the  $\frac{1}{2}^+$  (left) and  $F_i^-$  for the  $\frac{1}{2}^-$  (right) in the  $p! K^0 +$ .

$I(\theta)$  are given by

$$\begin{aligned}
 I^+(\theta) &= \mathcal{F}_1^+ \mathcal{J}^2 + \mathcal{F}_2^+ \mathcal{J}^2 - 2\text{Re}(\mathcal{F}_1^+ \mathcal{F}_2^+) \cos\theta + \sin^2\theta \\
 &\quad + \frac{1}{2}(\mathcal{F}_3^+ \mathcal{J}^2 + \mathcal{F}_4^+ \mathcal{J}^2) + \text{Re}(\mathcal{F}_1^+ \mathcal{F}_4^+ + \mathcal{F}_2^+ \mathcal{F}_3^+ + \mathcal{F}_3^+ \mathcal{F}_4^+ \cos\theta); \\
 I^-(\theta) &= \mathcal{F}_1^- \mathcal{J}^2 + \mathcal{F}_2^- \mathcal{J}^2 - 2\text{Re}(\mathcal{F}_1^- \mathcal{F}_2^-) \cos\theta + \sin^2\theta \\
 &\quad + \frac{1}{2}(\mathcal{F}_3^- \mathcal{J}^2 \sin^2\theta + \mathcal{F}_4^- \mathcal{J}^2) + \text{Re}(\mathcal{F}_1^- \mathcal{F}_3^- + \mathcal{F}_2^- \mathcal{F}_4^- - \mathcal{F}_2^- \mathcal{F}_3^- \cos\theta); \quad (5)
 \end{aligned}$$

As before, the angular distributions near threshold can be written as  $I^+(\theta) \sim \mathcal{F}_1^+ \mathcal{J}^2 + \frac{1}{2} \sin^2\theta \mathcal{F}_3^+ \mathcal{J}^2$  and  $I^-(\theta) \sim \mathcal{F}_1^- \mathcal{J}^2 + \frac{1}{2} \sin^2\theta \mathcal{F}_4^- \mathcal{J}^2$ , respectively. Then, from the discussion above the leading contributions of  $n! K^0 +$  lead to  $I^+(\theta) \sim \mathcal{F}_1^+ \mathcal{J}^2$  for the positive, and  $I^-(\theta) \sim \frac{1}{2} \sin^2\theta \mathcal{F}_4^- \mathcal{J}^2$  for the negative parity  $\frac{1}{2}^-$ . Consequently the positive parity will produce the s-wave behavior of  $\frac{d}{d\theta}^+$  and the negative parity yields a typical p-wave profile of  $\frac{d}{d\theta}^-$  near threshold. Similarly, we can write  $I^+(\theta) \sim \mathcal{F}_1^+ \mathcal{J}^2$  for the positive and  $I^-(\theta) \sim \mathcal{F}_1^- \mathcal{J}^2$  for the negative parity  $\frac{1}{2}^-$  in the process  $p! K^0 +$  near threshold. Due to the common s-wave nature of these amplitudes, however, the angular distributions in this case will be flat and therefore are not sensitive to the sign of the  $\frac{1}{2}^-$  parity. Thus, for the case of  $p! K^0 +$  we agree with Ref. [15] that one should analyze the multiply polarized process to distinguish between the positive and negative parity of  $\frac{1}{2}^-$ .

To illustrate explicitly, we presented the angular distributions for the positive and negative parity  $\frac{1}{2}^-$  states in Figs. 3 and 4. In the figures the angular distributions of  $n! K^0 +$  and  $p! K^0 +$  are calculated in the PV coupling scheme with coupling constants given in Table II [18]. The solid line is the contribution of the Born terms and notations for other lines are the same

as Ref. [18]. To reduce the model dependence arising from the form factors further, we presented the normalized angular distributions divided by the total cross section. As can be seen in Fig. 3 the solid lines of  $n \rightarrow K^+ \theta^+$  near threshold, i.e. at  $E_\gamma = 1.8$  GeV, show the typical s-wave kaon production of the Born terms for  $^+(\frac{1}{2}^+)$  and the p-wave distribution of the Born terms for  $^+(\frac{1}{2}^-)$ , respectively. These are consistent with the consequence of the parity and angular momentum conservation incorporated with the threshold kinematics of the production amplitude. Furthermore, such contrasting features of  $n \rightarrow K^+ \theta^+$  are not degraded by the model dependence especially due to the  $K$  and  $K_1$  contributions near threshold,  $E_\gamma = 1.8$  GeV. Therefore, the angular distribution of  $n \rightarrow K^+ \theta^+$  near threshold should provide the useful information on the parity of  $\theta^+$  without using the polarized photon beam and/or other polarized observables for that purpose. In Fig. 4 the enhancement of the backward angle rather than at in the solid line of  $\frac{d}{d\theta}^+$  is due to the u-channel contribution and this forward backward asymmetry is also observed in the neutral pion production on proton [28] by the similar reason. These analyses confirm our earlier discussions.

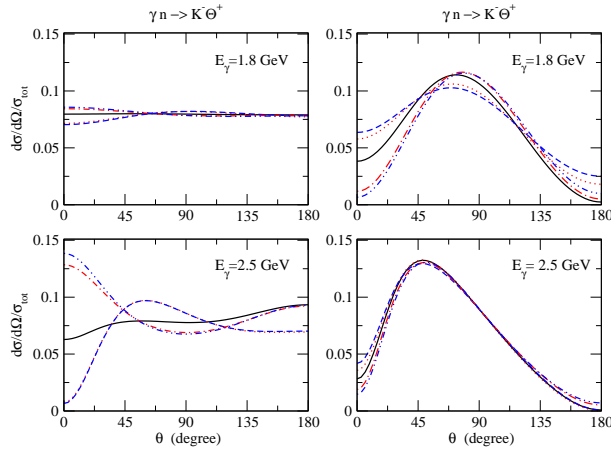


FIG. 3: Normalized angular distributions  $\frac{1}{\sigma} \frac{d\sigma}{d\Omega}$  of the  $^+(\frac{1}{2}^+)$  (left) and the  $^+(\frac{1}{2}^-)$  (right) for  $n \rightarrow K^+ \theta^+$  at  $E_\gamma = 1.8$  and 2.5 GeV.

### 3. Photon Polarization Asymmetry

It is natural to extend our prediction to the polarization observable, photon polarization asymmetry. Zhao [16] and Zhao and Akhalili [17] carried out analyses of  $\theta^+$  photoproduction with polarized photon beams using a quark potential model and examined kinematical and dynamical

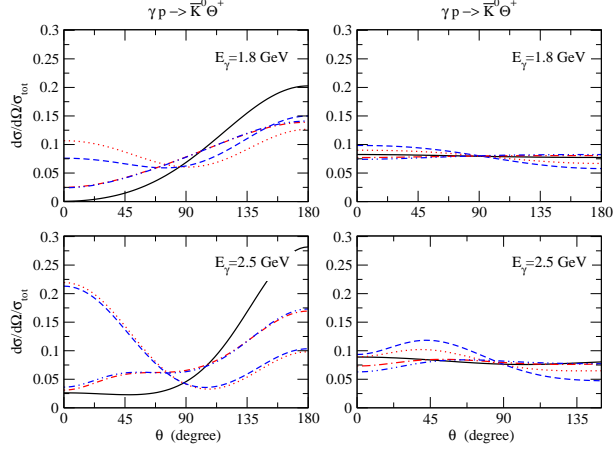


FIG. 4: Normalized angular distributions  $\frac{1}{\sigma} \frac{d^2\sigma}{d\theta d\phi}$  of the  $p^+$  ( $\frac{1}{2}^+$ ) (left) and the  $p^+$  ( $\frac{1}{2}^-$ ) (right) for  $p \rightarrow K^0 p^+$  at  $E_\gamma = 1.8$  and  $2.5$  GeV.

aspects for the purpose of determining  $p^+$  spin and parity. Although the model in Ref. [16] is different from ours, we notice that our results are rather close to the results of Ref. [16] in some cases supporting our findings in this work. The asymmetry from the photon polarization ( $\epsilon$ ) is defined by an interference between the spin- $\frac{1}{2}$  and the spin non- $\frac{1}{2}$  transitions, thus, enhancing the effect of the small part of the reaction amplitude and the properties hidden in the unpolarized characteristics can be revealed.

Following the convention given in Ref. [29], we choose the photon momentum  $\mathbf{k}$  in Eqs.(1) and (2) along the z-axis and the vector  $(\mathbf{k} \times \mathbf{q})$  to be parallel to the y-axis in the center of mass frame of the reaction. Then, the photon polarization asymmetry is defined by

$$\epsilon = \frac{d\sigma_{\text{pol}}^{\text{?}} - d\sigma_{\text{pol}}^{\text{k}}}{d\sigma_{\text{pol}}^{\text{?}} + d\sigma_{\text{pol}}^{\text{k}}}; \quad (6)$$

where  $d\sigma_{\text{pol}}^{\text{?}}$  ( $d\sigma_{\text{pol}}^{\text{k}}$ ) is the angular distribution for the photon polarization along x (y) axis. In terms of the CGLN amplitudes, the photon polarization for each parity of the  $p^+$  is given by

$$\begin{aligned} \epsilon^+ &= \frac{\sin^2 \theta}{2I^+(\theta)} [\mathcal{F}_3^+ \mathcal{J}^2 + \mathcal{F}_4^+ \mathcal{J}^2 + 2\text{Re}(\mathcal{F}_1^+ \mathcal{F}_4^+ + \mathcal{F}_2^+ \mathcal{F}_3^+ + \mathcal{F}_3^+ \mathcal{F}_4^+ \cos \theta)]; \\ &= \frac{\sin^2 \theta}{2I^+(\theta)} [\mathcal{F}_3^+ \mathcal{J}^2 \sin^2 \theta + \mathcal{F}_4^+ \mathcal{J}^2 + 2\text{Re}(\mathcal{F}_1^+ \mathcal{F}_3^+ + \mathcal{F}_2^+ \mathcal{F}_4^+ - \mathcal{F}_2^+ \mathcal{F}_3^+ \cos \theta)]; \end{aligned} \quad (7)$$

respectively.

With the angular distributions  $I^+(\theta)$  taken as before, the photon polarization asymmetry for  $p \rightarrow K^0 p^+$  near threshold can be approximated as  $\epsilon^+ \approx \frac{\sin^2 \theta}{2\mathcal{F}_1^+ \mathcal{J}^2} \mathcal{F}_3^+ \mathcal{J}^2 \approx 0$  for the positive parity substantially by the dominance of  $\mathcal{F}_1^+$  over  $\mathcal{F}_3^+$  as discussed in Section 2. Similarly the polarization for the negative parity can be given as  $\epsilon^- \approx \frac{\sin^2 \theta}{2\frac{1}{2}\sin^2 \theta \mathcal{F}_4^+ \mathcal{J}^2} \mathcal{F}_4^+ \mathcal{J}^2 \approx 1$  by the leading contribution

of  $F_4$ . In short, the polarization for  $n \rightarrow K^+ \left(\frac{1}{2}\right)$  near threshold can be characterized by such contrasting features between the  $^+ = 0$  due to the dominance of the  $K$  roll-Radem term and  $^+ = 1$  due to the  $t$ -channel kaon pole term, which are very sensitive to the parity of  $^+$ . Let us note that these features are resulted from the dominance of  $F_1^+$  and of  $F_4$  dictated by the conservation of parity and angular momentum plus the threshold kinematics as discussed in Section 2.

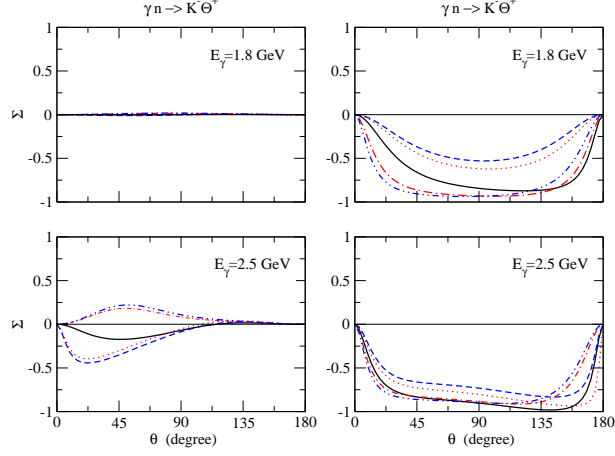


FIG. 5: Polarized photon asymmetries  $^+$  (left) and  $^+$  (right) for  $n \rightarrow K^+$  at  $E_\gamma = 1.8$  and  $2.5$  GeV.

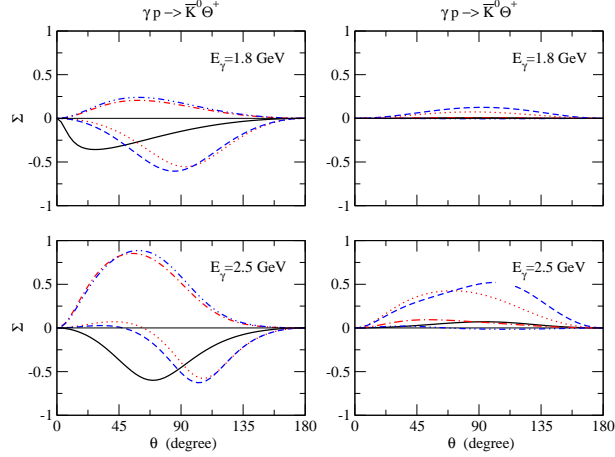


FIG. 6: Polarized photon asymmetries  $^+$  (left) and  $^+$  (right) for  $p \rightarrow K^0$  at  $E_\gamma = 1.8$  and  $2.5$  GeV.

The photon polarization asymmetries are calculated as before and the results are presented in Figs. 5 and 6 for  $n \rightarrow K^+$  and  $p \rightarrow K^0$ , respectively. Again, the notations for the lines are the same as in Ref. [18]. In Fig. 5 we found that what we discussed above is in good agreement with the solid lines of near threshold. Moreover, as the distinction of

between the two parity states near threshold is not much contaminated by the model-dependent contributions of  $K$  and  $K_1$ , the observation of  $\sigma$  for  $n \rightarrow K^+ \pi^+$  can serve for the determination of the  $\pi^+$  parity. For  $p \rightarrow K^0 \pi^+$ , the polarization  $P_{\parallel} = 0$  which appeared in the case of the negative parity  $\pi^+$  can be predicted by the dominance of  $F_1$  over  $F_4$ , i.e.,  $P_{\parallel} = \frac{\sin^2 \theta}{2F_1^2} F_4^2 = 0$ . This feature of the solid line maintains up to  $E = 2.5 \text{ GeV}$  as shown in Fig. 6. However, due to the common s-wave nature of both parities as mentioned above [15], the polarization in the case of  $p \rightarrow K^0 \pi^+$  is not sensitive to the parity of  $\pi^+$  as shown in the figures.

#### 4. Summary and discussion

In summary, we have analyzed the angular distribution and the photon polarization symmetry for  $N \rightarrow K^+ \pi^+$  process. The analysis presented here has demonstrated that the threshold amplitudes are dominated by the s- and p-wave multipole for the positive and negative parity  $\pi^+$ , respectively, in the case of  $n \rightarrow K^+ \pi^+$  process. Therefore, the measurement of the angular distribution and photon polarization asymmetry for  $n \rightarrow K^+ \pi^+$  can provide distinctive features to determine the  $\pi^+$  parity unambiguously. However, the situation is quite different in the case of  $p \rightarrow K^0 \pi^+$  process because the charge coupling of photon to the neutral meson is absent. Due to the indifferent nature of the angle dependence of threshold amplitude, the measurement of those observables for  $p \rightarrow K^0 \pi^+$  is not sensitive to the parity state of  $\pi^+$ . Taking into account the threshold kinematics of the CGLN amplitude, we can further show the consistency of our description. The features of the angular distribution and the photon polarization asymmetry seem to follow the natural consequence of the parity and angular momentum conservation applied to the threshold amplitude.

#### Acknowledgments

This work was supported in part by 2003 Hankuk Aviation university Faculty Research Grant and in part by a grant from the U.S. Department of Energy (DE-FG 02-96ER 40947).

---

[1] LEPS Collaboration, T. Nakano et al., Phys. Rev. Lett. 91, 012002 (2003).

[2] SAPHIR Collaboration, J. Barth et al., Phys. Lett. B 572, 127 (2003).

- [3] CLAS C Collaboration I, S. Stepanyan et al, Phys. Rev. Lett. 91, 252001 (2003).
- [4] CLAS C Collaboration II, V. Kubarovsky et al, Phys. Rev. Lett. 92, 032001 (2004).
- [5] DIANA C Collaboration, V. V. Barmin et al, Phys. Atom. Nucl. 66, 1715 (2003).
- [6] A. E. Akratyan, A. G. Dolgolenko, and M. A. Kubantsev, hep-ex/0309042.
- [7] HERMES C Collaboration, A. Arapetian et al, Phys. Lett. B 585, 213 (2004).
- [8] SVD C Collaboration, A. Aleev et al, hep-ex/0401024.
- [9] R. Jaffe and F. W. Ilczek, Phys. Rev. Lett. 91, 232003 (2003)  
D. Borisyuk, M. Faber, and A. Kobushkin, hep-ph/0307370.  
B. K. Jennings and K. Maltman, Phys. Rev. D 69, 094020 (2004).  
C. E. Carlson, C. D. Carone, H. J. Kwee, and V. Nazaryan, Phys. Lett. B 573, 101 (2003); Phys. Lett. B 579, 52 (2004).  
F. L. Stancu and D. O. Riska, Phys. Lett. B 575, 242 (2003).  
A. Hosaka, Phys. Lett. B 571, 55 (2003).  
L. Ya. Golzman, Phys. Lett. B 575, 18 (2003); hep-ph/0309092.  
M. Karliner and H. J. Lipkin, Phys. Lett. B 575, 249 (2003).
- [10] S.-L. Zhu, Phys. Rev. Lett. 91, 232002 (2003).  
R. D. Matheus, F. S. Navarra, M. Nielsen, R. da Silva, and S. H. Lee, Phys. Lett. B 578, 323 (2003).  
J. Sugiyama, T. Doi, and M. Oka, Phys. Lett. B 581, 167 (2004).  
F. C. Sikor, Z. Fodor, S. D. Katz, and T. G. Kovacs, JHEP 0311, 070 (2003); hep-lat/0309090.  
S. Sasaki, hep-lat/0310014.
- [11] A. W. Thomas, K. Hicks, and A. Hosaka, Prog. Theor. Phys. 111, 291 (2004).
- [12] C. Hanhart, M. Buscher, W. Eyrich, K. Kiklian, U.-G. Meiner, F. Rathmann, A. Sibirtsev, and H. Stroher, Phys. Lett. B 590, 39 (2004); hep-ph/0407107.
- [13] C. Hanhart, J. Haidenbauer, K. Nakayama, U.-G. Meiner, hep-ph/0407107.
- [14] K. Nakayama and W. G. Love, Phys. Rev. C 70, 012201 (2004); hep-ph/0404011.
- [15] M. P. Rekab, and E. Tomasi-Gustafsson, J. Phys. G 30, 1459 (2004); hep-ph/0401050.
- [16] Q. Zhao, Phys. Rev. D 69, 053009 (2004).
- [17] Q. Zhao and J. S. Alkhalili, Phys. Lett. B 585, 91 (2004).
- [18] B. G. Yu, T. K. Choi, and C.-R. Ji, Phys. Rev. C 70, 045205 (2004); nucl-th/0312075.
- [19] D. Drechsel, and L. Tiator, J. Phys. G 18, 449-497 (1992).
- [20] A. Donnachie, High Energy Physics vol. V, (edited by E. H. S. Burhop) Academic Press, 1972.
- [21] C. F. Chew, M. L. Goldberg, R. E. Low, and Y. Nambu, Phys. Rev. 106, 1345 (1957).
- [22] B. Kerbikov, and F. Tabakin, Phys. Rev. C 62, 064601 (2000).
- [23] E. Marco, E. Oset, and H. Toki, Phys. Rev. C 60, 015202 (1999).
- [24] W. Liu, C. M. Ko, and V. Kubarovsky, Phys. Rev. C 69, 025202 (2004); nucl-th/0312075.
- [25] <http://pdg.lbl.gov/pdg.html>
- [26] R. A. Williams et al, Phys. Rev. C 46, 1617 (1992).

- [27] K. Haglin, *Phys. Rev. C* 50, 1688 (1994).
- [28] O. Hanstein, D. D. Rechsel, and L. T. Iator, *Nucl. Phys. A* 632, 561 (1998).  
M. Fuchs et al., *Phys. Lett. B* 368, 20 (1996).
- [29] C. G. Fasano, F. Tabakin, and B. Saghai, *Phys. Rev. C* 46, 2430 (1992).